Small Angle J/ψ Production in $p\bar{p}$ Collisions at $\sqrt{s} = 1.8$ TeV

B. Abbott,[40] M. Abolins,[37] V. Abramov,[15] B. S. Acharya,[8] I. Adam,[39] D. L. Adams,[48] M. Adams,[24] S. Ahn,[23] H. Aihara,[17] G. A. Alves,[2] N. Amos,[36] E. W. Anderson,[30] R. Astur,[42] M. M. Baarmand,[42] V. V. Babintsev,[15] L. Babukhadia,[16] A. Baden,[33] V. Balamurali,[28] B. Baldin,[23] S. Banerjee,[8] J. Bantly,[45] E. Barberis,[17] P. Baringer,[31] J. F. Bartlett,[23] A. Belyaev,[14] S. B. Beri,[6] I. Bertram,[26] V. A. Bezzubov,[15] P. C. Bhat,[23] V. Bhatnagar,[6] M. Bhattacharjee,[42] N. Biswas,[28] G. Blazey,[25] S. Blessing,[21] P. Bloom,[18] A. Boehnlein,[23] N. I. Bojko,[15] F. Borcherding,[23] C. Boswell,[20] A. Brandt,[23] R. Breedon,[18] R. Brock,[37] A. Bross,[23] D. Buchholz,[26] V. S. Burtovoi,[15] J. M. Butler,[34] W. Carvalho,[2] D. Casey,[37] Z. Casilum,[42] H. Castilla-Valdez,[11] D. Chakraborty,[42] S.-M. Chang,[35] S. V. Chekulaev,[15] L.-P. Chen,[17] W. Chen,[42] S. Choi,[10] S. Chopra,[36] B. C. Choudhary,[20] J. H. Christenson,[23] M. Chung,[24] D. Claes,[38] A. R. Clark,[17] W. G. Cobau,[33] J. Cochran,[20] L. Coney,[28] W. E. Cooper,[23] C. Cretsinger,[41] D. Cullen-Vidal,[45] M. A. C. Cummings,[25] D. Cutts,[45] O. I. Dahl,[17] K. Davis,[16] K. De,[46] K. Del Signore,[36] M. Demarteau,[23] D. Denisov,[23] S. P. Denisov,[15] H. T. Diehl,[23] M. Diesburg,[23] G. Di Loreto,[37] P. Draper,[46] Y. Ducros,[5] L. V. Dudko,[14] S. R. Dugad,[8] A. Dyshkant,[15] D. Edmunds,[37] J. Ellison,[20] V. D. Elvira,[42] R. Engelmann,[42] S. Eno,[33] G. Eppley,[48] P. Ermolov,[14] O. V. Eroshin,[15] V. N. Evdokimov,[15] T. Fahland,[19] M. K. Fatyga,[41] S. Feher,[23] D. Fein,[16] T. Ferbel,[41] G. Finocchiaro,[42] H. E. Fisk,[23] Y. Fisyak,[43] E. Flattum,[23] G. E. Forden,[16] M. Fortner,[25] K. C. Frame,[37] S. Fuess,[23] E. Gallas,[46] A. N. Galyaev,[15] P. Gartung,[20] V. Gavrilov,[13] T. L. Geld,[37] R. J. Genik II,[37] K. Genser,[23] C. E. Gerber,[23] Y. Gershtein,[13] B. Gibbard,[43] B. Gobbi,[26] B. Gómez,[4] G. Gómez,[33] P. I. Goncharov,[15] J. L. González Solís,[11] H. Gordon,[43] L. T. Goss,[47] K. Gounder,[20] A. Goussiou,[42] N. Graf,[43] P. D. Grannis,[42] D. R. Green,[23] H. Greenlee,[23] S. Grinstein,[1] P. Grudberg,[17] S. Grünendahl,[23] G. Guglielmo,[44] J. A. Guida,[16] J. M. Guida,[45] A. Gupta,[8] S. N. Gurzhiev,[15] G. Gutierrez,[23] P. Gutierrez,[44] N. J. Hadley,[33] H. Haggerty,[23] S. Hagopian,[21] V. Hagopian,[21] K. S. Hahn,[41] R. E. Hall,[19] P. Hanlet,[35] S. Hansen,[23] J. M. Hauptman,[30] D. Hedin,[25] A. P. Heinson,[20] U. Heintz,[23] R. Hernández-Montoya,[11] T. Heuring,[21] R. Hirosky,[24] J. D. Hobbs,[42] B. Hoeneisen,[4,*] J. S. Hoftun,[45] F. Hsieh,[36] Ting Hu,[42] Tong Hu,[27] T. Huehn,[20] A. S. Ito,[23] E. James,[16] J. Jaques,[28] S. A. Jerger,[37] R. Jesik,[27] T. Joffe-Minor,[26] K. Johns,[16] M. Johnson,[23] A. Jonckheere,[23] M. Jones,[22] H. Jöstlein,[23] S. Y. Jun,[26] C. K. Jung,[42] S. Kahn,[43] G. Kalbfleisch,[44] D. Karmanov,[14] D. Karmgard,[21] R. Kehoe,[28] M. L. Kelly,[28] S. K. Kim,[10] B. Klima,[23] C. Klopfenstein,[18] W. Ko,[18] J. M. Kohli,[6] D. Koltick,[29] A. V. Kostritskiy,[15] J. Kotcher,[43] A. V. Kotwal,[39] A. V. Kozelov,[15] E. A. Kozlovsky,[15] J. Krane,[38] M. R. Krishnaswamy,[8] S. Krzywdzinski,[23] S. Kuleshov,[13] S. Kunori,[33] F. Landry,[37] G. Landsberg,[45] B. Lauer,[30] A. Leflat,[14] J. Li,[46] Q. Z. Li-Demarteau,[23] J. G. R. Lima,[3] D. Lincoln,[23] S. L. Linn,[21] J. Linnemann,[37] R. Lipton,[23] F. Lobkowicz,[41] S. C. Loken,[17] A. Lucotte,[42] L. Lueking,[23] A. L. Lyon,[33] A. K. A. Maciel,[2] R. J. Madaras,[17] R. Madden,[21] L. Magaña-Mendoza,[11] V. Manankov,[14] S. Mani,[18] H. S. Mao,[23,†] R. Markeloff,[25] T. Marshall,[27] M. I. Martin,[23] K. M. Mauritz,[30] B. May,[26] A. A. Mayorov,[5] R. McCarthy,[42] J. McDonald,[21] T. McKibben,[24] J. McKinley,[37] T. McMahon,[44] H. L. Melanson,[23] M. Merkin,[14] K. W. Merritt,[23] C. Miao,[45] H. Miettinen,[48] A. Mincer,[40] C. S. Mishra,[23] N. Mokhov,[23] N. K. Mondal,[8] H. E. Montgomery,[23] P. Mooney,[4] M. Mostafa,[1] H. da Motta,[2] C. Murphy,[24] F. Nang,[16] M. Narain,[23] V. S. Narasimham,[8] A. Narayanan,[16] H. A. Neal,[36] J. P. Negret,[4] P. Nemethy,[40] D. Norman,[47] L. Oesch,[36] V. Oguri,[3] E. Oliveira,[2] E. Oltman,[17] N. Oshima,[23] D. Owen,[37] P. Padley,[48] A. Para,[23] Y. M. Park,[9] R. Partridge,[45] N. Parua,[8] M. Paterno,[41] B. Pawlik,[12] J. Perkins,[46] M. Peters,[22] R. Piegaia,[1] H. Piekarz,[21] Y. Pischalnikov,[29] B. G. Pope,[37] H. B. Prosper,[21] S. Protopopescu,[43] J. Qian,[36] P. Z. Quintas,[23] R. Raja,[23] S. Rajagopalan,[43] O. Ramirez,[24] S. Reucroft,[35] M. Rijssenbeek,[42] T. Rockwell,[37] M. Roco,[23] P. Rubinov,[26] R. Ruchti,[28] J. Rutherfoord,[16] A. Sánchez-Hernández,[11] A. Santoro,[2] L. Sawyer,[32] R. D. Schamberger,[42] H. Schellman,[26] J. Sculli,[40] E. Shabalina,[14] C. Shaffer,[21] H. C. Shankar,[8] R. K. Shivpuri,[7] M. Shupe,[16] H. Singh,[20] J. B. Singh,[6] V. Sirotenko,[25] E. Smith,[44] R. P. Smith,[23] R. Snihur,[26] G. R. Snow,[38] J. Snow,[44] S. Snyder,[43] J. Solomon,[24] M. Sosebee,[46] N. Sotnikova,[14] M. Souza,[2] A. L. Spadafora,[17] G. Steinbrück,[44] R. W. Stephens,[46] M. L. Stevenson,[17] D. Stewart,[36] F. Stichelbaut,[42] D. Stoker,[19] V. Stolin,[13] D. A. Stoyanova,[15] M. Strauss,[44] K. Streets,[40] M. Strovink,[17] A. Sznajder,[2] P. Tamburello,[33] J. Tarazi,[19] M. Tartaglia,[23] T. L. T. Thomas,[26] J. Thompson,[33] T. G. Trippe,[17] P. M. Tuts,[39] V. Vaniev,[15] N. Varelas,[24] E. W. Varnes,[17] D. Vititoe,[16] A. A. Volkov,[15] A. P. Vorobiev,[15] H. D. Wahl,[21] G. Wang,[21] J. Warchol,[28] G. Watts,[45] M. Wayne,[28] H. Weerts,[37] A. White,[46] J. T. White,[47] J. A. Wightman,[30] S. Willis,[25] S. J. Wimpenny,[20] J. V. D. Wirjawan,[47] J. Womersley,[23] E. Won,[41] D. R. Wood,[35] Z. Wu,[23,†] H. Xu,[45] R. Yamada,[23] P. Yamin,[43] T. Yasuda,[35] P. Yepes,[48] K. Yip,[23] C. Yoshikawa,[22] S. Youssef,[21] J. Yu,[23] Y. Yu,[10]

B. Zhang,[23,†] Y. Zhou,[23,†] Z. Zhou,[30] Z. H. Zhu,[41] M. Zielinski,[41] D. Zieminska,[27] A. Zieminski,[27] E. G. Zverev,[14] and A. Zylberstejn[5]

(D0 Collaboration)

[1]*Universidad de Buenos Aires, Buenos Aires, Argentina*
[2]*LAFEX, Centro Brasileiro de Pesquisas Físicas, Rio de Janeiro, Brazil*
[3]*Universidade do Estado do Rio de Janeiro, Rio de Janeiro, Brazil*
[4]*Universidad de los Andes, Bogotá, Colombia*
[5]*DAPNIA/Service de Physique des Particules, CEA, Saclay, France*
[6]*Panjab University, Chandigarh, India*
[7]*Delhi University, Delhi, India*
[8]*Tata Institute of Fundamental Research, Mumbai, India*
[9]*Kyungsung University, Pusan, Korea*
[10]*Seoul National University, Seoul, Korea*
[11]*CINVESTAV, Mexico City, Mexico*
[12]*Institute of Nuclear Physics, Kraków, Poland*
[13]*Institute for Theoretical and Experimental Physics, Moscow, Russia*
[14]*Moscow State University, Moscow, Russia*
[15]*Institute for High Energy Physics, Protvino, Russia*
[16]*University of Arizona, Tucson, Arizona 85721*
[17]*Lawrence Berkeley National Laboratory and University of California, Berkeley, California 94720*
[18]*University of California, Davis, California 95616*
[19]*University of California, Irvine, California 92697*
[20]*University of California, Riverside, California 92521*
[21]*Florida State University, Tallahassee, Florida 32306*
[22]*University of Hawaii, Honolulu, Hawaii 96822*
[23]*Fermi National Accelerator Laboratory, Batavia, Illinois 60510*
[24]*University of Illinois at Chicago, Chicago, Illinois 60607*
[25]*Northern Illinois University, DeKalb, Illinois 60115*
[26]*Northwestern University, Evanston, Illinois 60208*
[27]*Indiana University, Bloomington, Indiana 47405*
[28]*University of Notre Dame, Notre Dame, Indiana 46556*
[29]*Purdue University, West Lafayette, Indiana 47907*
[30]*Iowa State University, Ames, Iowa 50011*
[31]*University of Kansas, Lawrence, Kansas 66045*
[32]*Louisiana Tech University, Ruston, Louisiana 71272*
[33]*University of Maryland, College Park, Maryland 20742*
[34]*Boston University, Boston, Massachusetts 02215*
[35]*Northeastern University, Boston, Massachusetts 02115*
[36]*University of Michigan, Ann Arbor, Michigan 48109*
[37]*Michigan State University, East Lansing, Michigan 48824*
[38]*University of Nebraska, Lincoln, Nebraska 68588*
[39]*Columbia University, New York, New York 10027*
[40]*New York University, New York, New York 10003*
[41]*University of Rochester, Rochester, New York 14627*
[42]*State University of New York, Stony Brook, New York 11794*
[43]*Brookhaven National Laboratory, Upton, New York 11973*
[44]*University of Oklahoma, Norman, Oklahoma 73019*
[45]*Brown University, Providence, Rhode Island 02912*
[46]*University of Texas, Arlington, Texas 76019*
[47]*Texas A&M University, College Station, Texas 77843*
[48]*Rice University, Houston, Texas 77005*

(Received 28 July 1998)

This paper presents the first measurement of inclusive J/ψ production cross section in the forward pseudorapidity region $2.5 \leq |\eta^{J/\psi}| \leq 3.7$ in $p\overline{p}$ collisions at $\sqrt{s} = 1.8$ TeV. The results are based on 9.8 pb^{-1} of data collected using the D0 detector at the Fermilab Tevatron Collider. The inclusive J/ψ cross section for transverse momenta between 1 and 16 GeV/c is compared with theoretical models of charmonium production. [S0031-9007(98)08183-6]

PACS numbers: 13.85.Ni, 12.38.Qk

In high energy $p\overline{p}$ collisions J/ψ's are produced directly, from decays of higher mass charmonium states [χ and $\psi(2S)$], and from b quark decays. Existing experimental results in the central rapidity region from UA1 [1] at $\sqrt{s} = 0.63$ TeV, and from CDF [2] and D0 [3] at $\sqrt{s} = 1.8$TeV demonstrate that then measured inclusive J/ψ transverse momentum distribution cannot be described solely by contributions from b quark decays and prompt production predicted by the color singlet model [4]. In the color singlet model the charmonium meson retains the quantum numbers of the produced $c\overline{c}$ pair and thus each J/ψ state can only be directly produced via the corresponding hard scattering color singlet subprocess. The model predicts direct J/ψ and $\psi(2S)$ production rates 50 times smaller than those observed by CDF [2]. To explain this discrepancy, a color octet model was introduced [5–7]. The color octet mechanism extends the color singlet approach by taking into account the production of $c\overline{c}$ pairs in a color octet configuration accompanied by a gluon. The color octet state evolves into a color singlet state via emission of a soft gluon. The parameters of the model were derived from a fit to CDF data for direct J/ψ and $\psi(2S)$ production at central rapidity. In this article we utilize the large rapidity coverage of the D0 muon system to study the process $p\overline{p} \to J/\psi + X \to \mu^+\mu^- + X$ in previously unexplored kinematical regions of small J/ψ transverse momenta and large rapidities. We compare our results with theoretical predictions extended into this kinematic domain.

The D0 detector [8] consists of three main systems: central and forward drift chambers, used to identify charged tracks for pseudorapidity $|\eta| \leq 3.2$; the uranium-liquid argon calorimeter with nearly hermetic coverage for $|\eta| \leq 4$; and the muon system. The detector component most relevant to this analysis is the small angle muon spectrometer (SAMUS) [9,10] consisting of magnetized iron toroids and drift tube stations on each side of the interaction region with pseudorapidity coverage of $2.2 < |\eta^\mu| < 3.3$ for a single muon.

The SAMUS stations, three in each arm, consist of three planes of 29 mm diameter drift tubes: vertical, horizontal, and inclined at 45°. The list of tubes containing hits is sent to the trigger system and drift times are used for offline track reconstruction. Muon track reconstruction is based on a Kalman fit [11] to the three-dimensional coordinates of muons passing through the SAMUS stations, one before the toroidal magnet and two after, and the coordinates of the event vertex. The muon momentum resolution σ_p/p is about 20%, limited by SAMUS coordinate resolution and by Coulomb scattering in the calorimeter and muon toroid.

The data were collected using the multilevel trigger system. The level 0 trigger [12] is used to select single interaction events with hits in scintillator hodoscopes situated on both sides of the interaction region. At the level 1 [13], signals from individual SAMUS tubes are OR'ed to provide 12 cm wide hodoscopic elements. The trigger requires a pattern of hits in the trigger elements consistent with at least one muon with transverse momentum $p_T^\mu > 3$ GeV/c coming from the interaction region. Because of high tube occupancy ($\simeq$4%) by soft electrons and positrons, we implement a "multiplicity cut" at the level 1 trigger. This cut rejects an event if the number of hit trigger elements in a vertically oriented tube plane exceeds a fixed threshold.

The logic of the level 1.5 trigger is similar to that of the level 1 trigger, but is based on better spatial segmentation (1.5 vs 12 cm). Events which pass the level 1.5 trigger are digitized and sent to the level 2 software trigger implemented on a farm of VAX stations, where reconstruction of muon tracks without using drift times is performed. The calorimeter information is used in the level 2 trigger to confirm the muon through its energy deposition.

Even with the multiplicity cut, the counting rates of the level 1 and level 1.5 triggers are high in comparison with the allocated trigger bandwidth. To further reduce counting rates, we use prescales up to 10 for the dimuon trigger.

In the offline analysis, we select events with one interaction vertex, a single muon or dimuon trigger, and at least two reconstructed muon tracks. Each muon candidate is required to have at least 15 hits on a track out of an average of 18. The energy deposition in the cells of the hadronic calorimeter along the muon track is required to exceed 1.5 GeV, and to be spread contiguously among all five calorimeter layers. To ensure a good momentum measurement, we require $p^\mu \leq 150$ GeV/c and a minimum traverse magnetic field integral of 1.2 T·m. In total, 1779 events with opposite sign muon pairs and 281 events with same sign muon pairs are selected from the data sample with integrated luminosity of 9.8 ± 0.5 pb^{-1} [14]. The estimated fraction of background tracks from accidental hit combinations in the final data sample is below 1%.

The opposite sign dimuon invariant mass distribution $M_{\mu\mu}$ for events with transverse momentum in the range $1.0 \leq p_T^{\mu\mu} \leq 16$ GeV /c and pseudorapidity $2.5 \leq |\eta^{\mu\mu}| \leq 3.7$ is shown in Fig. 1. In addition to the J/ψ signal, other contributions to the dimuon spectrum with $M_{\mu\mu} < 9$ GeV/c^2 are expected to come from $b\overline{b}$ and $c\overline{c}$ production (jointly denoted as $q\overline{q}$) with the heavy quarks decaying semileptonically or via sequential semileptonic decays, Drell-Yan production (DY), decay of light mesons (e.g., ρ, ϕ, η), and π or K decays.

To estimate the background and simulate the J/ψ detection efficiency, we use a sample of Monte Carlo (MC) events from the PYTHIA 5.7 [15] and JETSET [16] MC generators for each of the dimuon processes mentioned above, except π and K decays. The J/ψ events are generated (assuming no J/ψ polarization) with $p_T^{J/\psi}$ from 1 to 20 GeV/c and $|\eta^{J/\psi}|$ between 2.0 and 4.0. Generated dimuon events are simulated using D0 GEANT [17] and mixed with minimum bias events from the data to simulate the combinatoric background. These simulated

dimuon events are then subjected to a full trigger simulation and processed with the standard D0 reconstruction program.

Based on MC studies we approximate the J/ψ signal by a Gaussian function of $1/M_{\mu\mu}$ to account for limited muon momentum resolution. The mass spectrum in Fig. 1 is fit by the sum of the J/ψ signal (with the width and mean value as free parameters) and MC mass distributions for background processes (with free normalization). The number of events due to π and K decays is estimated from the data using like-sign dimuon events. The fit yields 691 ± 41 J/ψ events with mean mass $\langle M_{\mu\mu}\rangle = 3.03 \pm 0.03$ GeV/c^2, and standard deviation $\sigma_M = 0.56 \pm 0.03$ GeV/c^2.

The dimuon mass resolution does not allow a clear separation of the J/ψ and $\psi(2S)$ states. The fit of the invariant mass distribution yields a 90% C.L. upper limit of the $\psi(2S)$ fraction in the signal associated with the J/ψ of 15%. A direct measurement of inclusive $\psi(2S)$ production for $|\eta^{\psi}| < 0.6$ performed by CDF [2] shows that the J/ψ differential cross section is approximately 13 times larger than that of the $\psi(2S)$.

The inclusive differential cross section of J/ψ production is calculated from

$$\frac{d^2\sigma(\langle p_T^i\rangle, \langle|\eta^j|\rangle)}{dp_T^i d\eta^j} = \frac{1}{L\varepsilon_{ij}} \frac{N_{ij}}{\Delta p_T^i \Delta\eta^j},$$

where L is the total integrated luminosity, ε_{ij} is the J/ψ detection efficiency, and N_{ij} is the number of J/ψ events in the Δp_T^i, $\Delta\eta^j$ interval.

To calculate the number of J/ψ events, the fit to the mass spectrum is performed in five $\eta^{\mu\mu}$ and nine $p_T^{\mu\mu}$ intervals. To reduce the errors of the fit in the high $p_T^{\mu\mu}$ bins, the $p_T^{\mu\mu}$ dependence of the fraction of events attributed to J/ψ is fit to a linear function and the results of this fit are used to obtain the number of J/ψ events.

The efficiency of J/ψ detection includes acceptance, trigger efficiency, reconstruction efficiency, and offline cuts, and is given by

$$\varepsilon_{ij} = \frac{N(p_T^i, \eta^j)\,\varepsilon_{\rm cor}}{N_{\rm tot}(p_T^i, \eta^j)},$$

where $N(p_T^i, \eta^j)$ is the number of events in a given p_T^i, η^j bin which passed all selection criteria, $N_{\rm tot}(p_T^i, \eta^j)$ is the total number of generated events in a bin, and $\varepsilon_{\rm cor}$ is the correction factor for effects not simulated in MC. The $\varepsilon_{\rm cor}$ includes efficiencies for the level 2 trigger calorimeter confirmation of $(91 \pm 2)\%$ for the dimuon trigger and $(95 \pm 1)\%$ for the single muon trigger, and for offline cuts not simulated by the MC of $(79 \pm 4)\%$. Efficiencies for those cuts are obtained from the data and include $(88 \pm 1)\%$ for the single vertex cut, $(94 \pm 3)\%$ for the energy deposition cut, and $(96 \pm 2)\%$ for the cut on the number of hits on a track.

The measured J/ψ spectrum is unfolded to correct for the momentum and pseudorapidity smearing using the technique of Ref. [18]. The correction factors vary from 1.7 at low $p_T^{J/\psi}$ to 0.4 for $p_T^{J/\psi} > 8$ GeV/c.

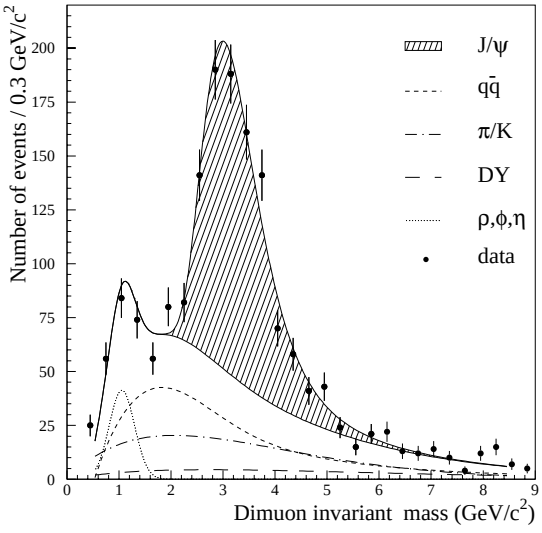

FIG. 1. The invariant mass spectrum of opposite sign dimuons with $1.0 \le p_T^{\mu\mu} \le 16$ GeV/c and $2.5 \le |\eta^{\mu\mu}| \le 3.7$. The hatched area indicates the J/ψ signal above the sum of the backgrounds.

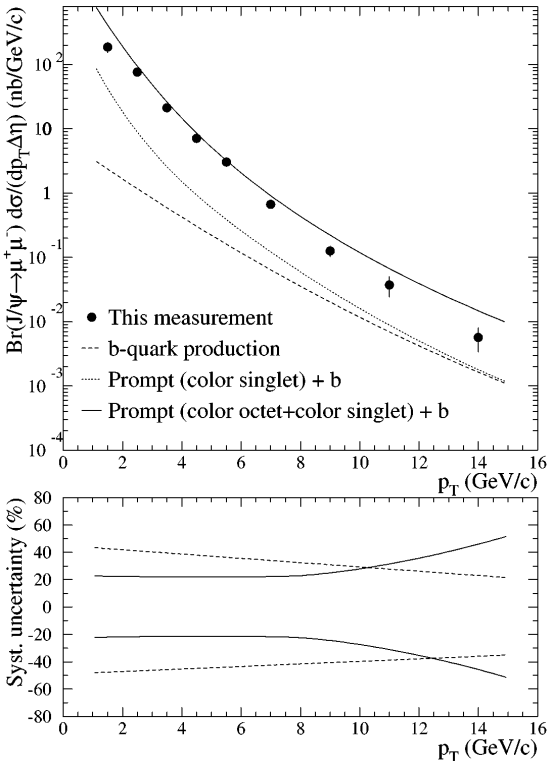

FIG. 2. The p_T dependence of the J/ψ differential cross section and its theoretical predictions (upper figure). Only the statistical errors are shown. The lower figure presents systematic uncertainties; the solid curves are the sum of all systematic errors, the dashed curves represent the uncertainty band due to J/ψ polarization. The upper (lower) dashed curve corresponds to 100% transverse (longitudinal) polarization.

TABLE I. J/ψ inclusive differential cross sections $Br(J/\psi \to \mu^+\mu^-)d^2\sigma/dp_T d\eta$ (nb/GeV/c).

$p_T^{J/\psi}$ (GeV/c)	$\eta^{J/\psi}$	2.5−3.7	2.65	2.95	3.25	3.55
1.5		187 ± 34	⋯	137 ± 55	183 ± 57	130 ± 45
2.5		77 ± 8	⋯	69 ± 18	69.9 ± 8.1	45.7 ± 5.3
3.5		21.3 ± 2.1	21.4 ± 6.4	23.8 ± 2.8	17.6 ± 2.0	15.6 ± 1.7
4.5		7.14 ± 0.77	7.9 ± 1.7	8.06 ± 0.83	5.59 ± 0.86	5.40 ± 0.83
5.5		3.03 ± 0.36	4.20 ± 0.65	3.22 ± 0.36	2.44 ± 0.46	⋯
7.0		0.667 ± 0.075	1.07 ± 0.13	0.758 ± 0.076	0.77 ± 0.16	⋯
9.0		0.126 ± 0.023	0.212 ± 0.033	0.132 ± 0.021	0.131 ± 0.039	⋯
11.0		0.037 ± 0.013	0.086 ± 0.020	0.050 ± 0.014	⋯	⋯
14.0		0.0057 ± 0.0023	0.0206 ± 0.0039	0.0064 ± 0.0020	⋯	⋯

The calculated differential cross section is fit to an exponential function. The results are used for interpolation of the cross sections from average values of $\langle p_T^i \rangle$ and $\langle |\eta^j| \rangle$ to the centers of the selected intervals. The inclusive differential J/ψ cross section averaged over a rapidity range of $2.5 \leq |\eta^{J/\psi}| \leq 3.7$ is shown in Fig. 2. Results for finer rapidity bins are collected in Table I. The uncertainties quoted there are statistical only.

The largest (>2%) systematic uncertainties are summarized in Table II. The contribution from the unfolding is derived from comparison with the bin-by-bin unfolding technique [19]. The uncertainties in the determination of the background and averaging cross section over the SAMUS pseudorapidity acceptance vary for different $p_T^{J/\psi}$ and are caused by uncertainties in the parametrization of the data. The difference in the parameters of measured and generated J/ψ mass distributions as well as the accuracy of the spectrometer description in the detector simulation are used to estimate the J/ψ detection efficiency uncertainty. The uncertainty due to the level 1 multiplicity cut was determined by varying the threshold of this cut by one trigger element. The results in Table I are obtained for the case of zero J/ψ polarization. The additional uncertainty up to $^{+40\%}_{-45\%}$ due to possible J/ψ polarization is shown in Fig. 2 along with the $p_T^{J/\psi}$ dependence of the total systematic error.

TABLE II. Systematic errors of the J/ψ cross sections.

Source	Systematic error
Unfolding procedure	15%
J/ψ background determination	7.2%–30%
J/ψ detection efficiency	7%
Level 1 multiplicity cut	6%
Total integrated luminosity	5.4%
$\psi(2S)$ contamination	$^{+0\%}_{-5\%}$
$d^2\sigma/dp_T d\eta$ total	20%–36%
Averaging over $2.5 < \lvert\eta^{J/\psi}\rvert < 3.7$	5%–30%
$d\sigma/dp_T \Delta\eta$ total	21%–47%

In Fig. 2 we compare the J/ψ cross section with current models of charmonium production. For J/ψ from b quarks we use the next-to-leading-order QCD predictions [20] with the renormalization/factorization scale $\mu = \frac{1}{3}\sqrt{m_b^2 + p_T^{b2}}$, where m_b and p_T^b are the parent b quark mass and transverse momentum, respectively. The scale is chosen to match theory predictions to the published D0 b quark cross sections in the central rapidity region [3]. We use ISAJET [21] to fragment b quarks into J/ψ. The color octet and color singlet contributions to the direct J/ψ production and radiative χ decays are taken from Ref. [7]. The term representing the direct J/ψ production is increased by 12% to account for the contribution from $\psi(2S)$ decays [2].

Figure 3 shows the pseudorapidity dependence of the measured J/ψ cross section for $p_T^{J/\psi} > 5$ and 8 GeV/c along with the corresponding central rapidity measurements of D0 [3] and CDF [2]. Within uncertainties, the color octet model plus b quark decays describe the η dependence of the inclusive J/ψ production in the full rapidity region.

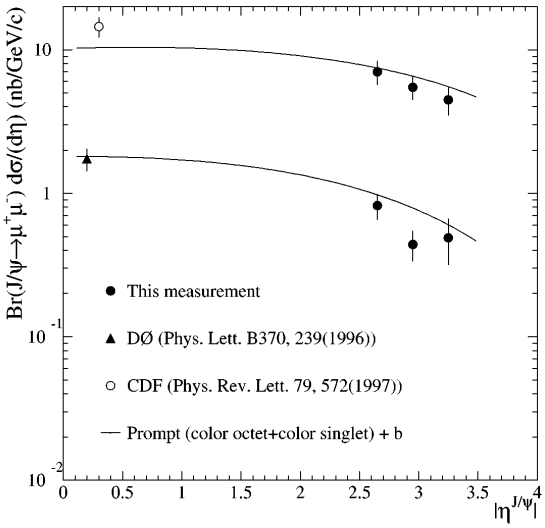

FIG. 3. The pseudorapidity dependence of the J/ψ production cross section with $p_T > 5$ GeV/c (upper points and curve) and $p_T > 8$ GeV/c (lower points and curve). The error bars

are statistical and systematic errors (polarization uncertainties not included) summed in quadrature.

In conclusion, we have made the first measurement of inclusive J/ψ production in the forward rapidity region $2.5 < |\eta^{J/\psi}| < 3.7$ in $p\overline{p}$ collisions at $\sqrt{s} = 1.8$ TeV. The data show good agreement with the theoretical predictions based on b quark decays and the color octet model of direct charmonium production.

We thank the staffs at Fermilab and collaborating institutions for their contributions to this work, and acknowledge support from the Department of Energy and National Science Foundation (U.S.), Commissariat à L'Energie Atomique (France), Ministry for Science and Technology and Ministry for Atomic Energy (Russia), CAPES and CNPq (Brazil), Departments of Atomic Energy and Science and Education (India), Colciencias (Colombia), CONACyT (Mexico), Ministry of Education and KOSEF (Korea), and CONICET and UBACyT (Argentina).

*Visitor from Universidad San Francisco de Quito, Quito, Ecuador.

†Visitor from IHEP, Beijing, China.

[1] UA1 Collaboration, C. Albajar *et al.*, Phys. Lett. B **256**, 112 (1991).

[2] CDF Collaboration, F. Abe *et al.*, Phys. Rev. Lett. **69**, 3704 (1992); **79**, 572 (1997); **79**, 578 (1997).

[3] D0 Collaboration, S. Abachi *et al.*, Phys. Lett. B **370**, 239 (1996).

[4] R. Baier and R. Ruckl, Z. Phys. C **19**, 251 (1983).

[5] E. Braaten and S. Fleming, Phys. Rev. Lett. **74**, 3327 (1995); P. Cho and M. Wise, Phys. Lett. B **346**, 129 (1995).

[6] M. Cacciari *et al.*, Phys. Lett. B **356**, 553 (1995).

[7] P. Cho and A. K. Leibovich, Phys. Rev. D **53**, 6203 (1996). The expected cross section for direct J/ψ production and the contribution from χ decays were calculated using code provided by P. Cho.

[8] D0 Collaboration, S. Abachi *et al.*, Nucl. Instrum. Methods Phys. Res., Sect. A **338**, 185 (1994).

[9] C. Brown *et al.*, Nucl. Instrum. Methods Phys. Res., Sect. A **279**, 331 (1989).

[10] Yu. Antipov *et al.*, Nucl. Instrum. Methods Phys. Res., Sect. A **297**, 121 (1990).

[11] P. Billoir, Nucl. Instrum. Methods Phys. Res., Sect. A **225**, 352 (1984).

[12] J. Bantly *et al.*, IEEE Trans. Nucl. Sci. **41**, 1274 (1994).

[13] M. Abolins *et al.*, Nucl. Instrum. Methods Phys. Res., Sect. A **289**, 543 (1990); M. Fortner *et al.*, IEEE Trans. Nucl. Sci. **38**, 480 (1991).

[14] J. Bantly *et al.*, Fermilab Technical Memo FNAL-TM-1995, 1997 (unpublished).

[15] T. Sjöstrand, Comput. Phys. Commun. **39**, 347 (1986); T. Sjöstrand and M. Bengtsson, Comput. Phys. Commun. **43**, 367 (1987).

[16] M. Bengtsson and T. Sjöstrand, Comput. Phys. Commun. **46**, 43 (1987).

[17] R. Brun and F. Carminati, CERN Program Library Long Writeup W5013, 1993 (unpublished); we use GEANT v3.15.

[18] G. D'Agostini, Nucl. Instrum. Methods Phys. Res., Sect. A **362**, 487 (1995).

[19] V. B. Anikeev, A. A. Spiridonov, and V. P. Zhigunov, Nucl. Instrum. Methods Phys. Res., Sect. A **322**, 280 (1992).

[20] The expected inclusive b quark cross section was calculated using the MNR code, provided by M. Mangano.

[21] F. Paige and S. Protopopescu, BNL Report No. 38304, 1986 (unpublished).